FACTA UNIVERSITATIS
Series: **Mechanical Engineering** Vol. 23, No 1, 2025, pp. 171 - 181
https://doi.org/10.22190/FUME250114012H

Original scientific paper

SURFACE ENERGY CHARACTERIZATION OF A SINGLE MICROSPHERE PARTICLE USING PEAKFORCE QUANTITATIVE NANOMECHANICAL MAPPING MODE OF ATOMIC FORCE MICROSCOPE

Heebo Ha[1], Sebastian Mueller[2],
Svetlana Guriyanova[2], Byungil Hwang[3]

[1]Department of Intelligent Semiconductor Engineering,
Chung-Ang University, Republic of Korea
[2]Material Science, BASF SE, Germany
[3]School of Integrative Engineering, Chung-Ang University, Republic of Korea

ORCID iDs: Heebo Ha https://orcid.org/0000-0003-3047-2263
Sebastian Mueller https://orcid.org/0009-0009-4843-1575
Svetlana Guriyanova https://orcid.org/0009-0007-2622-6787
Byungil Hwang https://orcid.org/0000-0001-9270-9014

Abstract. *The composites are typically created by embedding functional fillers in polymeric matrices. The key indicators of reliable performance include homogeneous filler dispersion and optimal interfacial properties between the fillers and matrix. Poor dispersion causes stress concentration, premature failure, and increased filler requirement for achieving functional properties like conductivity. Additionally, interfacial characteristics are governed by surface energy differences and significantly influence the mechanical properties like elongation and rupture stress. Conventional methods for measuring surface energy, such as contact angle or Washburn adsorption, have limitations when applied to microscale powders, including issuers with accurate size handling and bulk material requirements. To overcome these challenges, the PeakForce QNM (quantitative nanomechanical mapping) mode of atomic force microscopy (AFM) was used to measure the surface energy on the surface of the powder microspheres. This method was used to characterize the surface energies of 2–5 µm carbonyl iron powders with various surface coatings. Differences in the surface energies corresponded to variations in the dispersibility and mechanical performances of these powder-based composites. The proposed nanoscale approach provides critical insights into the interfacial mechanisms, enabling enhanced design and optimization of stetchable composites for advanced electronic applications.*

Key words: *Carbonyl iron powder, Composites, Surface energy, Contact angle, PeakForce quantitative nanomechanical mapping, Atomic force microscopy*

Received: January 14, 2025 / Accepted March 23, 2025

Corresponding author: Byungil Hwang
School of Integrative Engineering, Chung-Ang University, Seoul 06974, Republic of Korea
E-mail: bihwang@cau.ac.kr

1. INTRODUCTION

Given the increasing interest in flexible and stretchable electronics, there is increasing demand for compliant composites that are reliable under severe mechanical deformations [1-3]. The main strategy for fabricating such composites involves incorporating functional fillers along with the stretchable polymeric matrix [4-6]. Generally, these fillers are one- or two-dimensional materials that are dispersed in the polymer matrix via a homogenization process [7-9]. Depending on the physical properties of each component, these stretchable composites can be used in various applications [10-12]. In the fabrication of these composites, homogeneous dispersion of the fillers in the matrix is an important step for achieving highly stable stretchable composites [7, 13]. Agglomeration of the filler material can cause involuntary stress concentration that can result in failure of the composite at a much lower stress level than that expected for a composite with uniformly dispersed fillers [14, 15]. Furthermore, the amount of filler needed to achieve a certain level of functional properties, such as electrical conductivity or magnetic interference, can be much larger for composites with inhomogeneously dispersed fillers. Another factor that affects the physical stability of a stretchable composite is the characteristics of the interface between the filler surface and matrix [16, 17]. Depending on the status of interface formation, the mechanical properties of a composite such as its elongation or rupture stress is determined; thus, controlling the interfacial characteristics is crucial to obtaining the desired mechanical properties of stretchable composites [18, 19].

The dispersibility of a filler in a matrix as well as the interfacial characteristics between the filler and matrix are closely related to the differences in their surface energies [20, 21]. The higher wettability of a solid filler in a matrix indicates better dispersibility in the matrix [22, 23]. The method of measuring the contact angle using the sessile drop is the most common approach for obtaining the surface energies of each of the components in the composites [24, 25]. However, for microscale powders, the size of the liquid drop is larger than the particle size, which can cause errors in the surface energy calculations [26, 27]. The Washburn adsorption method is another option for evaluating the surface energy of a microscale powder [28], where the amount of liquid adsorbed on the powder is converted to the wetting ability of the powder, i.e., its surface energy [29]. However, group of agglomerated particles is required to measure the surface energy using the Washburn method; here, the surface energy of the individual particle is ignored even though it is important for understanding the detailed mechanisms of the changes in the mechanical properties of the composites. Hence, this method cannot be used for measuring hydrophobic (>90°) powders.

To overcome the limitations of the conventional surface energy characterization methods for microscale powders, the PeakForce quantitative nanomechanical mapping (PF-QNM) imaging mode of atomic force microscopy (AFM) was utilized. In the PF-QNM mode, the adhesion force is measured with nanometer resolution and converted into surface energy using a calibration curve established for well-known silane-coated surfaces [30, 31]. For example, Park et al. [32] characterized the surface energy of nanoscale Au strips using the AFM PF-QNM mode. This work revealed a relationship between adhesion force and contact angle at the nanoscale, representing a novel measurement method for challenging characterization of the nanoscale surface energy. In another work by Ha et al. [33], the grain size effect on the surface energy of metal thin film was investigated through PF-QNM method. However, there have been no attempts to characterize the surface energies of microscale powders. Herein, the surface energies of various carbonyl iron powders (CIPs) with diameters in the range of 2–5 μm and different hydrophobicities were characterized using the PF-QNM mode of AFM. Different surface coatings on the CIPs resulted in different surface energy values that could change the dispersibility in the composite states. The surface energies of individual microscale powders will enhance the understanding of the detailed mechanisms regarding the effects of interfacial characteristics on the mechanical properties of the CIP-based composites.

2. MATERIALS AND METHODS

2.1. Materials and Sample Fabrication

In this study, the commercially available carbonyl iron powders (BASF SE) of different grades (HQ, CC, and HQ-I) were used as received.

Additionally, the surface of HQ CIP was chemically modified by the different functionality. For this, the native oxide layer was needed to be removed, firstly. 100 g of HQ grade was added to 250 mL of 0.5 M hydrochloric acid (HCl; 35–37%, Daejung Chemical Co. Ltd.) and sonicated for 30 min. A permanent magnet was then used to settle the CIPs at the bottom of the container. The sedimented CIPs were later separated from the solvent and sequentially washed thrice with ethanol and deionized (DI) water for 15 min each.

To synthesize the CIP coated by tetraethyl orthosilicate (TEOS), ethanol and TEOS were mixed in a 7.6:1 ratio and reacted for a total volume of 200 mL. One drop of HCl was added to the mixture to create an acidic pH environment that acted as the catalyst. The sol-aging process was conducted by storing the mixture for 24 h to ensure full reaction development. The pretreated HQ grade with removed native oxide layer were added to the TEOS mixture and mechanically stirred at room temperature for 2 h, resulting in the formation of the SiO_2 layer on the CIP surfaces. The TEOS coated CIPs were settled at the bottom of the container by using a permanent magnet, and the solvent was removed. The HQ@TEOS particles were sequentially cleaned thrice with ethanol and DI water for 15 min each. Finally, the HQ@TEOS were dried in a vacuum oven at 120°C for 12 h to evaporate the remaining ethanol and water on their surfaces. All CIP grades and their particle size and chemical surface modification are listed in table 1.

To compare the conventional sessile drop method for determining the surface energy with the AFM PF-QNM technique, a PET substrate was coated with a 30 μm thick Acronal dispersion layer (BASF SE, Ludwigshafen, Germany) using a doctor blade. Afterwards, the CIPs were sprinkled onto the Acronal surface, and the unattached powder particles were removed by using a nitrogen blow gun.

To measure the adhesion force on CIP surface with nanometer resolution, the AFM PF-QNM technique needs a calibration curve to convert the adhesion data into a corresponding surface energy as well as contact angle. For this purpose, various self-assembled alkyl silane monolayers (SAMs) in a wide range of hydrophobicities were prepared on an ultra-flat silicon wafer. In a first instance, the silicon wafers were initially ultrasonic cleaned in a 1:1 mixture of acetone:ethanol for 15 min and subsequently dried under a nitrogen gas atmosphere. Moreover, the cleaned silicon wafers were treated with oxygen plasma (100 W) for 5 min to activate the surface for the chemical treatment. Directly after the plasma treatment, the clean and activated silicon wafers were immersed in a 2% silane/ anhydrous toluene solution for 15 min. Subsequently, the wafers were rinsed with toluene to remove any aggregates or contaminants. The SAM-treated silicon wafers were dried at 150 °C for 5 min on a hot plate.

Table 1 Carbonyl iron powder (CIP) grades and their average particle size and surface coating

Sample	Particle size (D50)	Coating
HQ	1.7 µm	No
HQ@TEOS	1.8 µm	TEOS modified
CC	4.3 µm	Silica
HQ-I	3.6 µm	I = Insulated

2.2. Characterization

The surface morphologies of the CIPs were analyzed using field-emission scanning electron microscopy (FESEM; S-3400 N, Hitachi). The particle sizes of the CIPs were determined using a particle size analyzer (PSA; Microtrac P3000, USA). Prior to measuring the particle sizes, calibrations were performed to eliminate the influence of ethanol. The contact angle and surface energy were measured with a drop shape analyzer (DSA100, Krüss, Germany) by using the sessile drop method. DI water, formamide and diiodomethane were used as solvents that represented the polar and nonpolar state, respectively. The surface roughness and adhesion force were measured by AFM (Dimension ICON microscope, Bruker, USA) with a standard silicon cantilever (RTESPA-300–125; Bruker, tip radius: 125 nm, spring constant: 40 N/m). To ensure a consistent tip force, the deflection sensitivity and spring constant were calibrated.

3. RESULTS AND DISCUSSION

Analyzing particles with different surface properties is a key step in the measurement of single-particle adhesion force at the nanoscale resolution. Although most of the particles have similar structures, their surface roughness and coating conditions tend to vary. Using PF-QNM, it was possible to analyze individual particles with surface energy across a broad range. The use of CIP particles that are commonly used in industries showed that it was possible to investigate diverse sample conditions with different coatings and surface roughness. The CIPs included HQ grade with a native oxide layer as well as silica- or insulate-coated grades, which enable comparisons using the conventional sessile drop method as well as other approaches. Additionally, particles with TEOS-modified surface functionalities and roughness were fabricated in this study.

Fig. 1 illustrates the SEM top-view, AFM topography and phase images of the different CIP grades with a varying particle size distribution, surface roughness, and coatings. In Fig. 1(a), and (b), after removing the native oxide layer of the HQ particles, they were coated with silica to produce the TEOS particles with similar sizes and shapes [34, 35]. Consequently, the TEOS particles coated with thin silica layers exhibited reduced surface roughness. The Ra roughness values (calculated from the 1µmx1µm AFM topography image) for the HQ grade were initially ~2.6 nm but decreased to ~2.2 nm for the TEOS particles. However, Fig. 1(c), and (d) showing silica or insulated coatings presented higher surface roughness; these rough and dotted surfaces resulted in Ra roughness values of 4.5, and 5.5 nm, respectively.

To measure the contact angles of the CIP particles with varying surface structures, the sessile drop method was used as the conventional measurement method. However, significant measurement errors were noted owing to time-dependent variations. The spreading rate of the solvent droplet was influenced by the particle hydrophilicity, which created challenges in obtaining precise contact angle measurements. Furthermore, as the droplet size was larger than the average particle size, there was additional complexity as the effects of both the particles and substrate (acrylic glue used for fixation) could not be disregarded.

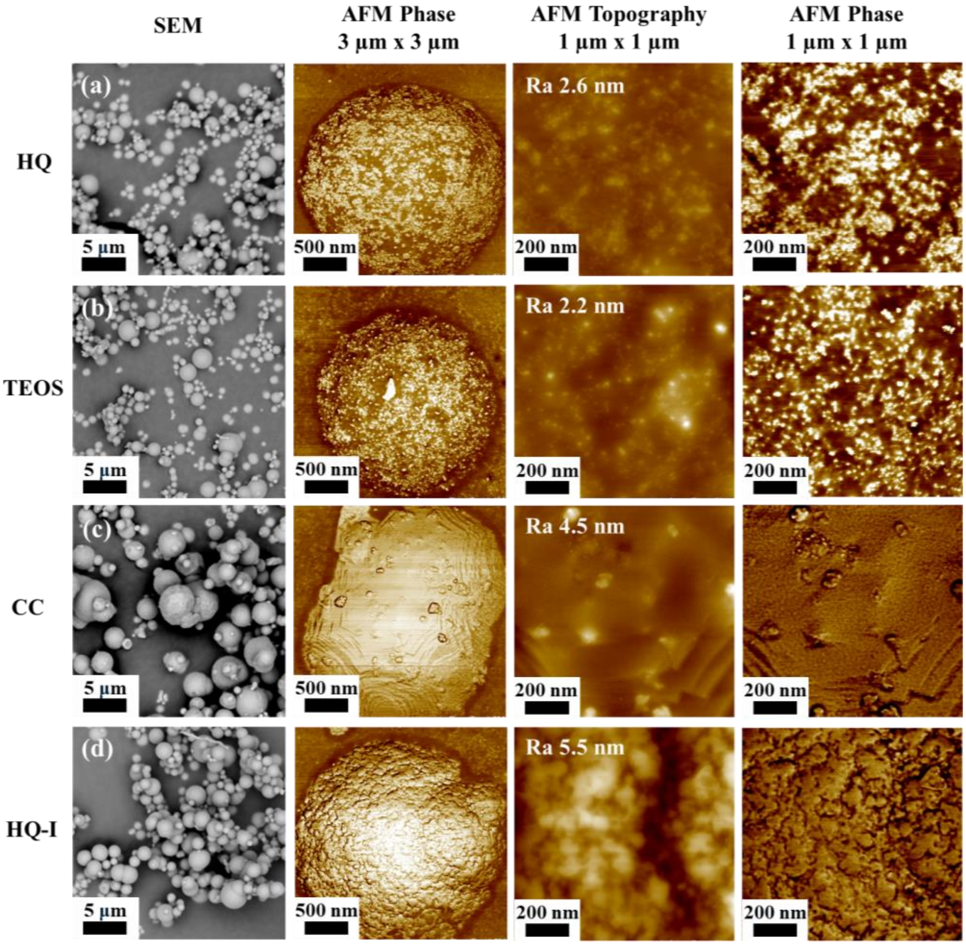

Fig. 1 The SEM top-view, AFM tapping mode topography and corresponding phase images show the particle distribution, surface structure and roughness of different CIP grades: (a) HQ, (b) TEOS-modified, (c) CC, and (d) HQ-I

Fig. 2 shows the changes in the contact angles over time from 0 to 30 s. The HQ grade particles showed relatively small reductions from 119° to 102°, while the CC and HQ-I grade particles showed steeper reductions from 78° to 58° as well as 43° to 17° over a dwell time of 30 s, respectively. These results represent the strong time dependency of the contact angle measurements, which can decrease the accuracy of the particle surface energy measurements.

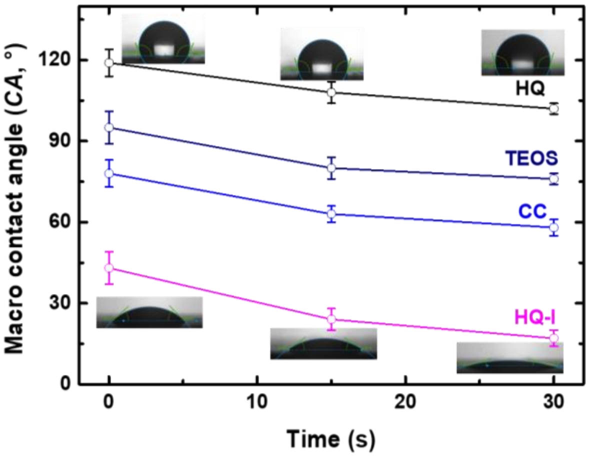

Fig. 2 Macro contact angle variation of CIP grades according to time measured by using the Krüss drop shape analyzer

The need for precise nanoscale measurements and particle-specific analysis is increasingly evident. The AFM PF-QNM mode offers a high-resolution method for characterizing the mechanical and chemical surface properties at the nanoscale. PF-QNM is an innovative AFM mode that uses low frequencies to periodically tap the peak force on the wanted area of the sample, allowing real-time recording of force versus separation curves. The peak force, representing the maximum vertical force applied to the sample surface, is recorded. In PF-QNM mode, the software calculates the force between the AFM tip and the sample surface based on feedback that reflects surface morphology and mechanical properties, so the peak force remains constant.

Fig. 3 presents a schematic illustration of the nanoscopic contact angle (*nCA*) measurement on micro-particles using AFM PF-QNM. The macroscopic wettability behavior is correlated with adhesion force and can be evaluated using the PF-QNM mode to calculate the contact angle and surface energy (*SE)* at the nanoscale. A variety of silane-modified silicon wafers are utilized as references to determine the *nCA* and *SE* across a wide hydrophilic-hydrophobic range. On these reference silane layers, the macroscopic contact angle and surface energy are obtained through the sessile drop method, while the adhesion force on silanes was measured using AFM to create the calibration curves (which will be explained later in the paper) with linear fit equations:

$$nCA = -4.4 \cdot F_{adh} + 185.2 \tag{1}$$

$$SE = 2.5 \cdot F_{adh} - 23.4 \tag{2}$$

where F_{adh} represents the adhesion force measured from the sample surface.

The types of silanes used, along with their corresponding macro contact angle, surface energy, and adhesion force values, are listed in Table 2. Subsequently, the contact angle and surface energy values of the microscale CIP particles are derived by comparing the measured adhesion forces with those from the previously established calibration curve.

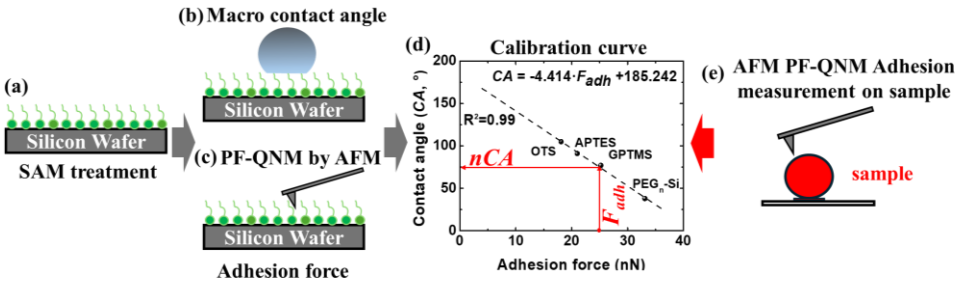

Fig. 3 Schematic illustration of the process to evaluate the nano contact angle or surface energy on micrometer sized CIP particle measured by the AFM PF-QNM technique

Table 2 Macro contact angles, surface energies, and adhesion forces of different alkyl silane types as reference system for the calibration curve

Silane type	Contact angle [°]	Surface energy [mN/m]	Adhesion force [nN]
Octyltrichlorosilane (OTS)	105	27	18
(3-Aminopropyl)triethoxysilan (APTES)	91	54	21
(3-Glycidyloxypropyl)trimethoxysilane (GPTMS)	77	42	25
Methoxy(polyethyleneoxy)propyl]triethoxysilane (PEG_n-Si)	38	61	33

The high-resolution topological AFM images of the surface of individual CIP particles are shown in Fig. 4. Variations in adhesion force are influenced by the surface structure, roughness and chemical groups. The particulate surface structure of each CIP grade, as shown in Fig. 4, was compared with the corresponding F_{adh} presented in Fig. 5, and the data were appropriately analyzed for the *nCA* and for the *SE* calculations.

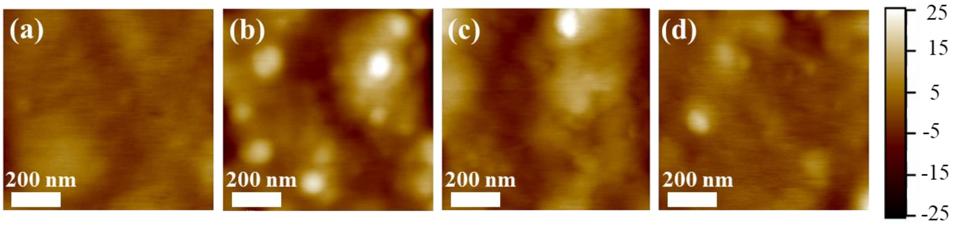

Fig. 4 AFM PF-QNM topography images on the surface of single CIP particle of different grades: (a) HQ, (b) TEOS-modified, (c) CC, and (d) HQ-I

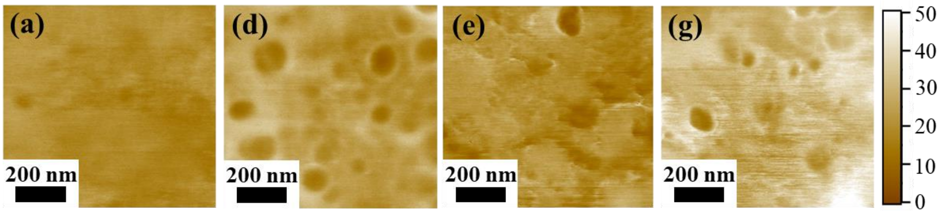

Fig. 5 AFM PF-QNM adhesion force images on the surface of single CIP particle of different grades: (a) HQ, (b) TEOS-modified, (c) CC, and (g) HQ-I

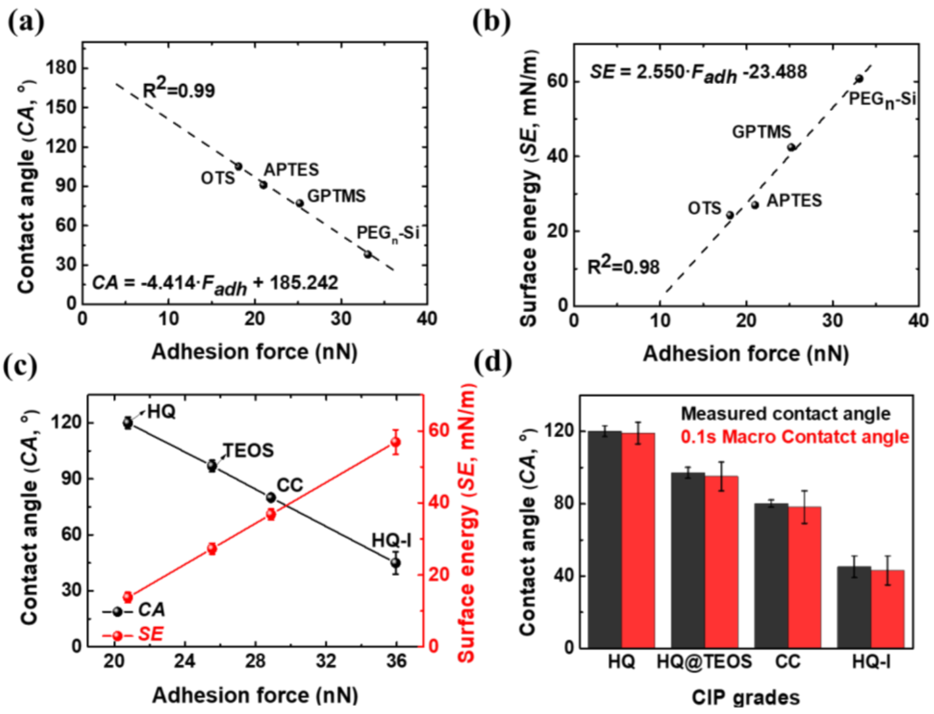

Fig. 6 Calibration curves according to adhesion forces from the different alkyl silane monolayers measured by AFM PF-QNM versus the (a) macro contact angle and (b) surface energy measured with the Krüss drop shape analyzer. (c) Adhesion forces measured on CIP surface versus the nano contact angle and surface energy calculated from the calibration curve. (d) Comparison of the nano and macro contact angle of the CIP grades measured with two different measuring systems – Krüss drop shape Analyzer versus AFM PF-QNM

Using the calibration curve given by Eqs. (1) and (2), the adhesion forces of the CIP particles with varying surface conditions and roughness from Fig. 5 were used to calculate the *nCA* and *SE* values, shown in Fig. 6(c) and (d). These results show high correlations between the adhesion forces and conventional macroscopic methods. The hydrophilicity of the silanes used for the calibration curves significantly influenced the F_{adh}, which was correlated with the *nCA* and *SE* (Figs. 6 (a) and (b)). The F_{adh} for single CIP particles were substituted into the equations to calculate the *nCA* and *SE* values. Fig. 6 (c) presents the *nCA* and *SE* values of single CIP particles with different surface conditions and roughness; this shows that hydrophobic particles exhibit lower F_{adh}, consistent with their higher *nCA*. Conversely, hydrophilic samples show higher F_{adh}, confirming that the F_{adh} are inversely proportional to *nCA* and directly proportional to *SE*. Fig. 6 (d) highlights the correlations between the macro contact angle measured at 0.1 s and the *nCA* values, showing their similarity. This indicates the potential applicability of the proposed method to similar types of particles, as it confirms the time intervals suitable for conventional techniques that evolve over time. Consequently, the proposed approach is anticipated to be extendable to a wide range of particle types.

The findings of this study demonstrate the feasibility of accurate nanoscale measurements and possibility of in-situ analysis of single particles. This study focused on the surface properties of single particles by assuming stable chemical structures. However, it also shows the possibility of in-situ analysis of chemically unstable particles or surfaces for future research endeavors.

4. CONCLUSIONS

In this study, the feasibility and effectiveness of using PF-QNM mode in AFM was demonstrated for characterizing the surface energies of individual microscale particles, specifically microscale CIPs. By overcoming the limitations of conventional methods such as the sessile drop and Washburn adsorption methods, the PF-QNM mode offers a nanoscale resolution approach to surface energy measurements. The results reveal that the surface energies vary significantly depending on the surface modification and roughness of the CIPs. These variations can directly influence the dispersibility of the particles in composite materials, thereby affecting their mechanical properties and functionalities. The correlations between adhesion force measurements and traditional contact angle methods validate the reliability of the PF-QNM approach. Additionally, the high-resolution insights provided by the proposed technique offer new possibilities for in-situ analyses of chemically or structurally unstable particles, extending its applicability to a broader range of materials and industries. The results of this study highlight the critical roles of interfacial characteristics in determining the mechanical performances of composites and underscore the value of advanced characterization techniques for optimizing the material properties. Future research could focus on applying PF-QNM to various particle systems and studying the potential for real-time monitoring of dynamic interfacial processes, including time-dependent changes in surface energy during particle interactions or aging. This approach deepens our understanding of time-dependent material behavior and allows for more precise control of the manufacturing process for advanced composites.

Acknowledgement: *This work was supported by the National Research Foundation of Korea (NRF) grant funded by the Korea government (MSIT) (RS-2024-00413272).*

REFERENCES

1. Rogers, J. A., Someya, T., Huang, Y., 2010, *Materials and mechanics for stretchable electronics*, Science, 327(5973), pp. 1603-1607.
2. Harris, K. D., Elias, A. L., Chung, H.-J., 2016, *Flexible electronics under strain: a review of mechanical characterization and durability enhancement strategies*, Journal of Materials Science, 51, pp. 2771-2805.
3. Almuslem, A. S., Shaikh, S. F., Hussain, M. M., 2019, *Flexible and stretchable electronics for harsh-environmental applications*, Advanced Materials Technologies, 4(9), 1900145.
4. Wang, D., Ren, S., Chen, J., Li, Y., Wang, Z., Xu, J., Jia, X., Fu, J., 2022, *Healable, highly thermal conductive, flexible polymer composite with excellent mechanical properties and multiple functionalities*, Chemical Engineering Journal, 430, 133163.
5. Choi, C., Qaiser, N., Hwang, B., 2024, *Mechanically pressed polymer-matrix composites with 3d structured filler networks for electromagnetic interference shielding application*, Facta Universitatis-Series Mechanical Engineering, 22, pp. 601-614.

6. Memarzadeh, A., Onyibo, E. C., Asmael, M., Safaei, B., 2024, *Dynamic effect of ply angle and fiber orientation on composite plates*, Spectrum of Mechanical Engineering and Operational Research, 1(1), pp. 90-110.
7. Kim, H., Kim, G., Kang, J. H., Oh, M. J., Qaiser, N., Hwang, B., 2025, *Intrinsically conductive and highly stretchable liquid metal/carbon nanotube/elastomer composites for strain sensing and electromagnetic wave absorption*, Advanced Composites and Hybrid Materials, 8(1), pp. 1-14.
8. Lavagna, L., Nisticò, R., Musso, S., Pavese, M., 2021, *Functionalization as a way to enhance dispersion of carbon nanotubes in matrices: A review*, Materials today chemistry, 20, 100477.
9. Hong, S., Qaiser, N., Ha, H., Hwang, B., 2024, *Enhanced stretchability of porous PDMS/CIP composites via weak interfacial bonding and their electromagnetic noise suppression properties*, Applied Surface Science, 664, 160200.
10. Yun, G., Tang, S.-Y., Lu, H., Zhang, S., Dickey, M. D., Li, W., 2021, *Hybrid-filler stretchable conductive composites: from fabrication to application*, Small Science, 1(6), 2000080.
11. He, X., Shi, J., Hao, Y., Wang, L., Qin, X., Yu, J., 2021, *PEDOT: PSS/CNT composites based ultra-stretchable thermoelectrics and their application as strain sensors*, Composites Communications, 27, 100822.
12. Das, P., Katheria, A., Jana, A., Das, M., Roy, B., Nayak, J., Nath, K., Ghosh, S. K., De, A., Das, N. C., 2023, *Super-stretchable, self-healing 2D MXene-based composites for thermal management and electromagnetic shielding applications*, ACS Applied Engineering Materials, 1(4), pp. 1186-1200.
13. Olonisakin, K., Fan, M., Xin-Xiang, Z., Ran, L., Lin, W., Zhang, W., Wenbin, Y., 2022, *Key improvements in interfacial adhesion and dispersion of fibers/fillers in polymer matrix composites; focus on pla matrix composites*, Composite Interfaces, 29(10), pp. 1071-1120.
14. Díez-Pascual, A. M., 2022, *PMMA-based nanocomposites for odontology applications: a state-of-the-art*, International Journal of Molecular Sciences, 23(18), 10288.
15. Marino, F., Pawlik, M., Valvano, S., 2024, *Mechanical Analysis of Sandwich Plates with Lattice Metal Composite Cores*, Spectrum of Mechanical Engineering and Operational Research, 1(1), pp. 44-63.
16. Kashfipour, M. A., Mehra, N., Zhu, J., 2018, *A review on the role of interface in mechanical, thermal, and electrical properties of polymer composites*, Advanced Composites and Hybrid Materials, 1, pp. 415-439.
17. Zhang, S., Wang, X., Yang, J., Chen, H., Jiang, X., 2023, *Micromechanical interlocking structure at the filler/resin interface for dental composites: a review*, International Journal of Oral Science, 15(1), 21.
18. Balazs, A. C., Emrick, T., Russell, T. P., 2006, *Nanoparticle polymer composites: where two small worlds meet*, Science, 314(5802), pp. 1107-1110.
19. Deng, H., Lin, L., Ji, M., Zhang, S., Yang, M., Fu, Q., 2014, *Progress on the morphological control of conductive network in conductive polymer composites and the use as electroactive multifunctional materials*, Progress in Polymer Science, 39(4), pp. 627-655.
20. Zhang, X., Li, B. W., Dong, L., Liu, H., Chen, W., Shen, Y., Nan, C. W., 2018, *Superior energy storage performances of polymer nanocomposites via modification of filler/polymer interfaces*, Advanced Materials Interfaces, 5(11), 1800096.
21. Stöckelhuber, K. W., Das, A., Jurk, R., Heinrich, G., 2010, *Contribution of physico-chemical properties of interfaces on dispersibility, adhesion and flocculation of filler particles in rubber*, Polymer, 51(9), pp. 1954-1963.
22. Bayat, A., Ebrahimi, M., Ardekani, S. R., Iranizad, E. S., Moshfegh, A. Z., 2021, *Extended Gibbs free energy and laplace pressure of ordered hexagonal close-packed spherical particles: A wettability study*, Langmuir, 37(28), pp. 8382-8392.
23. Harikrishnan, A., Das, S. K., Agnihotri, P. K., Dhar, P., 2017, *Particle and surfactant interactions effected polar and dispersive components of interfacial energy in nanocolloids*, Journal of Applied Physics, 122(5). 54301
24. Alghunaim, A., Kirdponpattara, S., Newby, B.-m. Z., 2016, *Techniques for determining contact angle and wettability of powders*, Powder Technology, 287, pp. 201-215.
25. Kozbial, A., Li, Z., Conaway, C., McGinley, R., Dhingra, S., Vahdat, V., Zhou, F., D'Urso, B., Liu, H., Li, L., 2014, *Study on the surface energy of graphene by contact angle measurements*, Langmuir, 30(28), pp. 8598-8606.
26. Susana, L., Campaci, F., Santomaso, A. C., 2012, *Wettability of mineral and metallic powders: applicability and limitations of sessile drop method and Washburn's technique*, Powder Technology, 226, pp. 68-77.
27. Kadyrov, R., Mukhamatdinov, I., Statsenko, E., 2023, *Determination of Sessile Drop Wetting Angle Based on μCT without the Direct Angle Measurement*, Langmuir, 39(8), pp. 2966-2973.
28. Wang, Z., Chu, Y., Zhao, G., Yin, Z., Kuang, T., Yan, F., Zhang, L., Zhang, L., 2023, *Study of surface wettability of mineral rock particles by an improved Washburn method*, ACS omega, 8(17), pp. 15721-15729.

29. Galet, L., Patry, S., Dodds, J., 2010, *Determination of the wettability of powders by the Washburn capillary rise method with bed preparation by a centrifugal packing technique*, Journal of Colloid and Interface Science, 346(2), pp. 470-475.
30. Adamcik, J., Lara, C., Usov, I., Jeong, J. S., Ruggeri, F. S., Dietler, G., Lashuel, H. A., Hamley, I. W., Mezzenga, R., 2012, *Measurement of intrinsic properties of amyloid fibrils by the peak force QNM method*, Nanoscale, 4(15), pp. 4426-4429.
31. Ha, H., Müller, S., Baumann, R.-P., Hwang, B., 2024, *Peakforce quantitative nanomechanical mapping for surface energy characterization on the nanoscale: A mini-review*, Facta Universitatis-Series Mechanical Engineering, 22, pp. 1-12.
32. Park, W., Müller, S., Baumann, R.-P., Becker, S., Hwang, B., 2020, *Surface energy characterization of nanoscale metal using quantitative nanomechanical characterization of atomic force microscopy*, Applied Surface Science, 507, 145041.
33. Ha, H., Ko, S., Goh, B., Müller, S., Baumann, R.-P., Leem, M., Jo Yoo, S., Choi, J., Hwang, B., 2022, Influence of Grain Boundary Density on the Surface Energy of Nanocrystalline Metal Thin Films, Applied Surface Science, 604, 154463.
34. Małecki, P., Kolman, K., Pigłowski, J., Kaleta, J., Krzak, J., 2015, *Sol–gel method as a way of carbonyl iron powder surface modification for interaction improvement*, Journal of Solid State Chemistry, 226, pp. 224-230.
35. Cvek, M., Moucka, R., Sedlacik, M., Pavlinek, V., 2017, *Electromagnetic, magnetorheological and stability properties of polysiloxane elastomers based on silane–modified carbonyl iron particles with enhanced wettability*, Smart Materials and Structures, 26(10), 105003.